Korean J. Chem. Eng., **22**(3), 433-440 (2005)

Study on the Mechanism of Hindered Sedimentation by 'Unified Theory on Solid-Liquid Separation'

Sung-Sam Yim† and Yun-Min Song

Department of Environmental Engineering, Inha University, Incheon 402-751, Korea
(*Received 23 July 2004 • accepted 2 March 2005*)

Abstract−The entire procedure of hindered sedimentation has been calculated by the introduction of new boundary conditions to the 'unified theory on solid-liquid separation.' During this study, the hindered sedimentation was defined as 'a process of sedimentation with transmission of the gravitational force between the particles due to contact.' The lower concentration limit, on which the 'unified theory on solid-liquid separation' is based, could not be applied. To understand the mechanism of hindered sedimentation, variations in the porosity during sedimentation were calculated by using our theory.

Key words: Hindered Sedimentation, Unified Theory on Solid-Liquid Separation, Solid-Liquid Separation

INTRODUCTION

Hindered sedimentation is widely used in solid-liquid separation because the energy consumption is small and the efficiency comparatively high. However, the detailed mechanism remains to be verified.

Richardson and Zaki [1954] proposed an experimental equation: "the velocity of a solid blanket at the beginning of hindered sedimentation was proportional to the terminal velocity of a free settling particle and also to the exponent 4.65 of the porosity." A further experimental equation was suggested by Maude and Whitmore [1958], which used the exponent 'n' instead of the 4.65 suggested by Richardson and Zaki, where the value of 'n' was determined by the particle Reynolds number (N_{Rep}). These two experimental equations are proposed for only the initial period of hindered sedimentation, where the velocity of the solid blanket is constant, and so do not have the theoretical background for explaining the phenomena during hindered sedimentation of sedimenting particulates.

Compared to the above two studies, Kynch's sedimentation theory [1952] offers, to some degree, an analysis of the phenomena of hindered sedimentation, as it is based on the phenomena during hindered sedimentation. However, Kynch's theory also considers the linear velocity during the initial period, but cannot give an explanation for the latter period when the velocity of the solid blanket continuously decreases.

Later, Tiller and Khatib [1984] analyzed the phenomena of hindered sedimentation, but their analysis was composed of a series of three different previously presented theories.

In this study, a theoretical calculation for hindered sedimentation was performed by using the 'unified theory on solid-liquid separation' previously proposed by the authors [Yim and Kwon, 1997]. The calculation was based on the conception that the new expression theory proposed by the author [Yim et al., 2003] could be applied to the hindered sedimentation theory. By applying new boundary conditions to the expression theory, the whole procedure of hindered sedimentation and the internal phenomena during sedimentation were calculated. A further purpose of this study was to find the lower concentration limit below which the 'unified theory on solid-liquid separation' would no longer be valuable.

†To whom correspondence should be addressed.
E-mail: yimsungsam@inha.ac.kr

THEORETICAL ANALYSIS

1. Fundamental Concepts

McCabe et al. [1995] suggested: "in hindered settling, the velocity gradients around each particles are affected by the presence of nearby particles." From this interpretation, the theoretical explanation for hindered sedimentation is very difficult. In this study, the hindered sedimentation has been defined as a sedimentation procedure with transmission of forces between solid particles. With transmitting forces, contact between particles is inevitable.

For a fairly thick suspension, it has been postulated that the contact between particles exists at the beginning of sedimentation, and due to this contact transmission of forces exists between particles, which then exert solid compressive pressure, p_s. However, at the start of sedimentation, the solid compressive pressure is considered small enough to be neglected.

The particles lying on the bottom are subjected to bottom solid compressive pressure, p_{sb}, exerted from the particles above. The p_{sb} value is initially very small, but increases as the sedimentation proceeds, and finally reaches a maximum due to the weight of the totally sedimented particles.

The solid compressive pressure at the solid blanket, i.e., the other side of the bottom, is called the 'upper solid compressive pressure,' p_{su}.

2. Theoretical Basis of Hindered Sedimentation

The authors [Yim and Kwon, 1997] proposed that the mechanisms of cake filtration, expression, hindered sedimentation, centrifugation, and centrifugal filtration can be explained by the same concept, with the differences between them occurring due to the operation conditions. In this study, the boundary conditions of hindered sedimentation were applied to the expression equations proposed by

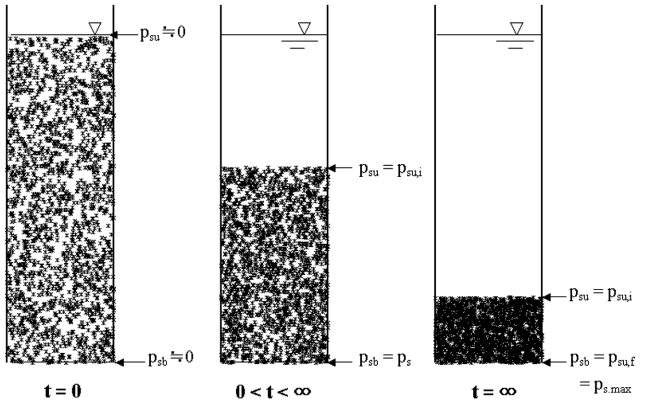

Fig. 1. Schematic diagram of hindered sedimentation.

the authors [Yim et al., 2003], based on the 'unified theory on solid-liquid separation.'

3. New Boundary Conditions in Hindered Sedimentation

The assumed procedure of hindered sedimentation is as shown in Fig. 1.

On the initiation of hindered sedimentation, i.e., t=0, the particles contact each other, but are all still floating in the liquid. Thus, the solid compressive pressure, p_s, in the direction of sedimentation is almost negligible.

When sedimentation begins, t>0, the weight of the particles is transferred in the direction of sedimentation and the solid compressive pressure of the particles on the bottom begins to increase. The p_{su}, which is the solid compressive pressure of the solids composing the solid blanket, is very small, and referred to as $p_{su,i}$. The $p_{su,i}$ was assumed to remain constant during the sedimentation procedure, but conversely, the p_{sb} to increase.

On completion of hindered sedimentation, t=∞, the p_{sb} reaches its largest value, p_{smax}, and originates from the total weight of particles. It was our assumption that the p_{su} remains at the value of $p_{su,i}$.

4. The Constitutive Equation for This Study

Another of our assumptions was that the equations shown in (1), i.e., the constitutive equations, obtained by using the Compression-Permeability Cell (CPC) developed by Ruth [1946] can be applied to very low solid compressive pressure, which is the first time this assumption has been made.

$$\alpha = a p_s^n \qquad 1-\varepsilon = B p_s^\beta \tag{1}$$

Yim et al. [2003] proved by sedimentation experiments that the equations shown in (1) were applicable to a very small solid compressive pressure of 0.01 Pa. It has also been suggested that the lower limit of this equation was 1 kPa [Tiller and Crump, 1977].

5. Sedimentation Velocity

The motive factor is the driving force for sedimenting particles during hindered sedimentation, and decreases in this factor the supporting force of solid particles at the bottom of the cell. This can be expressed as Eq. (2) using a modification of Darcy's equation.

$$v_o = \frac{\text{driving force} - \text{supporting force}}{\text{resistance}} = \frac{\text{driving force} - p_{sb}A}{\alpha_{av}\mu WA} \tag{2}$$

Here, v_o is the velocity of hindered sedimentation, A the cross-sectional area of sedimentation, α_{av} the average specific cake resistance of the sedimenting particles, μ the viscosity of liquid and W the total mass of solid particles per unit cross sectional area of sedimentation.

The gravity force of the particles minus the buoyant force of the solid particles in the liquid is the driving force for solid particles, which can be expressed as Eq. (3).

$$\begin{aligned}\text{driving force} &= \text{gravity force} - \text{buoyant force}\\ &= F_g - F_b = mg - \rho g V_s\\ &= mg - \frac{\rho}{\rho_s} mg\\ &= mg\left(1 - \frac{\rho}{\rho_s}\right)\end{aligned} \tag{3}$$

Here, m is the mass of solid particles [kg], ρ_s the density of solid particles [kg/m^3], ρ the density of liquid [kg/m^3] and V_s the volume of solid particles [m^3]. Substituting Eq. (2) into Eq. (3), and dividing by the cell cross sectional area, gives:

$$v_o = \frac{\left(1 - \frac{\rho}{\rho_s}\right) Wg - p_{sb}}{\alpha_{av}\mu W} \tag{4}$$

The density of liquid (ρ), solid particles (ρ_s) and the viscosity of liquid (μ) can be measured, with the mass of solid particles per unit area (W) not changing during hindered sedimentation, so this feature could also be measured. Thus, the instant velocity of hindered sedimentation, v_o, can be calculated by using Eq. (4) when the p_{sb} and average specific resistance, α_{av} are known.

6. Calculation of the Solid Compressive Pressure of the Particles on the Bottom, p_{sb}

To calculate the solid compressive pressure of the particles on the bottom, p_{sb}, at a given time, the definitions the 'average porosity' and the 'boundary conditions of hindered sedimentation' have also been proposed in this study. The 'average porosity, ε_{av},' is defined as:

$$\varepsilon_{av} = 1 - \frac{(\text{solid volume})}{(\text{volume below solid blanket})} \tag{5}$$

The solid volume can be calculated by dividing the mass of solid by the solid density (ρ_p), and the product of the cell area by the sedimentation height, L, which gives the total sedimentation volume, i.e., the volume below the solid blanket. This conception leads to;

$$\begin{aligned}\varepsilon_{av} &= 1 - \frac{(\text{solid mass})/(\text{solid density})}{(\text{area})(\text{sedimenting height})}\\ &= 1 - W\frac{1}{L\cdot\rho_s}\left(\frac{\text{kg}}{\text{m}^2\text{m}}\frac{\text{m}^3}{\text{kg}}\right)\end{aligned} \tag{6}$$

here, W is given by (solid mass)/(area), and L by (sedimenting height).

The equation introduced by Tiller and Crump [1977] for the average porosity leads to Eq. (7) when the new boundary condition proposed in this study is introduced.

$$\varepsilon_{av} = 1 - \frac{\int_{p_{su}}^{p_{sb}} \frac{dp_s}{\alpha}}{\int_{p_{su}}^{p_{sb}} \frac{dp_s}{\alpha(1-\varepsilon)}} \tag{7}$$

Then, Eq. (8) is obtained by substituting Eq. (7) into Eq. (1).

$$\varepsilon_{av} = 1 - \frac{1-n-\beta}{1-n} B \frac{p_{sb}^{1-n} - p_{su}^{1-n}}{p_{sb}^{1-n-\beta} - p_{su}^{1-n-\beta}} \quad (8)$$

As Eqs. (6) and (8) represent the same average porosity, and the combination of the two equations leads to:

$$L = \frac{W}{\rho_s} \frac{1-n}{1-n-\beta B} \frac{1}{p_{sb}^{1-n-\beta} - p_{su}^{1-n-\beta}} \quad (9)$$

Here, the compressive coefficients, n, B and β represent the characteristics of solid particles, and these values are determined by using the CPC. p_{sb} is the solid compressive pressure of the particles lying on the bottom, and p_{su} is that of the particles at the top. The value of p_{sb} at the sedimentation height, L, can be calculated by using this equation.

EXPERIMENTAL

1. Experimental Apparatus

A 500 mL cylinder, with an internal diameter of 4.61 cm, equipped with a measuring rule was used as the sedimentation cell. The heights of the solid blanket were measured with respect to time. The schematic diagram of the experimental apparatus for hindered sedimentation is shown in Fig. 2. Experiments, from low to high concentrations, were performed to find the relationship between the concentration and the rate of sedimentation. The final sedimentation height was determined by a 24 hour experiment.

2. Experimental Material

Several materials were considered for use in the experiment. For activated sludge, it was difficult to obtain the same quality for several experiments and impossible without changing the sedimentation characteristics. Thus, calcium carbonate ($CaCO_3$: Yakuri Pure Chemical Co.) was chosen as the experimental material.

The volumetric diameters of the particles were distributed uniformly between 0.2-60 μm, with a volumetric average diameter of 10.6 μm found using a Malvern Mastersizer. However, almost 10% of the particles were below 1 μm.

3. Precautions for the Experiments of Hindered Sedimentation

The factors influencing the sedimentation experiment are summarized as below:

(1) Sufficient mixing of suspension before sedimentation.
(2) Exclusion of the air existing inside and outside of the particles.
(3) Technique of inserting particles into liquid.
(4) Temperature difference between the outside and inside of the cell.
(5) Similarities in the diameters of cells between the top and bottom.
(6) Differences in the initial height of suspension.
(7) Flatness of the cell bottom and perpendicularity between the cell and ground.
(8) Particular diameter, shape, and size distribution.

Mixing before sedimentation has a great effect the experimental results. A uniform suspension must be made by mixing with sufficient intensity. The very small air bubbles within particles change the sedimentation velocity by reducing the overall density of the particles. To eliminate this air, the suspension was heated to 80 °C, cooled to room temperature and then agitated for 30 minutes with magnetic bars to provide a homogeneous suspension.

Prior to initiation of the sedimentation experiments, the method known as the 'invert method,' proposed by Alan and Justin [1962], was employed to give reproducibility. The 'invert method' involves inverting the sedimentation cell 8 to 10 times. Too much inverting is not desirable as air can be attached to the particles.

The differences in the diameters, and the variation in the initial height between the different batch tests were not critical factors. However, in the case of flow sedimentation, the so-called 'wall effect,' caused by a small diameter, could not be disregarded.

RESULTS AND DISCUSSION

1. Variation of the Calcium Carbonate Concentration

The experimental results for various solid contents, from 5.8 to 20.9 wt%, are shown in Fig. 3. For suspensions below 5.8 wt%, a solid blanket was not formed, so experiments for hindered sedimentation were not possible below this value. For the suspensions greater than 20.9 wt%, the sedimentation velocities were too slow for practical use.

The x-axis in Fig. 3 is the time divided by the initial sedimenta-

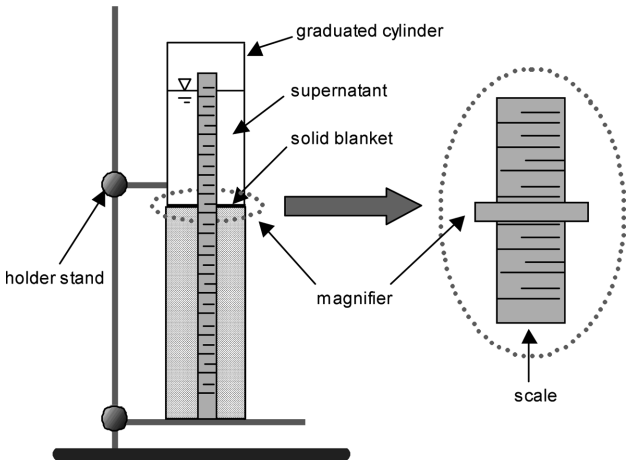

Fig. 2. Schematic diagram of the experimental apparatus for hindered sedimentation.

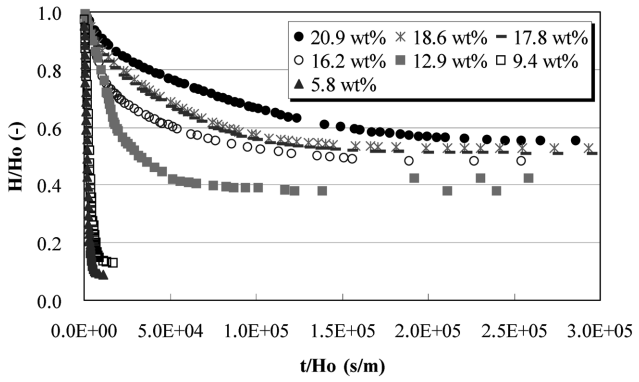

Fig. 3. Experimental results of hindered sedimentation from 5.8 to 20.9 wt% $CaCO_3$ suspension.

Table 1. The values of a, n, B and β from the sedimentation data for the 18.6 wt% $CaCO_3$ suspension

	Values
a	1.60×10^{9}
n	0.192
B	0.109
β	0.057

tion height, and y axis the height to the solid blanket from the bottom in relation to the initial height. There was a great difference between the experimental results for 9.4 and 12.9 wt%; these will be analyzed in detail later.

2. Determination of the Coefficients of Constitutive Equation

During hindered sedimentation, particles can loosely combine and the actual sedimenting particle size change. Thus, the particles formed will not have the same properties as measured by using the CPC. The values of n and β obtained by Grace [1953] with the CPC, and the value of B from our sedimentation results were adopted. With these values of n, β and B, the value of 'a' was chosen by comparing the experimental hindered sedimentation and theoretical calculated curve. The suspension concentration chosen for this operation was 18.6 wt%. The determined coefficients are shown in Table 1.

The values of a, n, B and β represent the characteristics of the calcium carbonate particles. The compressibility, n, was 0.192. Tiller and Horng [1983] defined that a compressibility of 0.2 as a "slightly compressible cake."

The results of the experimental hindered sedimentation and the calculation for the calcium carbonate suspension of 18.6 wt% are represented in Fig. 4.

The experimental and calculated results, from the beginning to the end of hindered sedimentation, were in good agreement. As stated above, a theory able to express the whole procedure of hindered sedimentation does not exist. Almost all previous theories have dealt with the initial period of sedimentation only. Despite the fairly thick suspension, with a short straight line portion during the initial period, our new theory can describe the whole procedure of hindered sedimentation.

Tiller and Khatib [1984] claimed that at least three independent theories were required to describe the whole hindered sedimentation procedure, but herein, the whole sedimentation procedure has

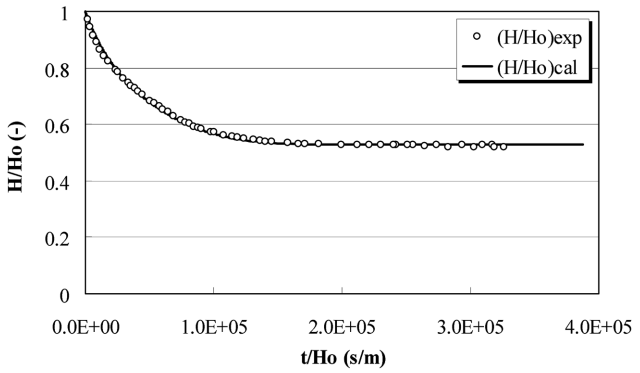

Fig. 4. Experimental and calculated results of hindered sedimentation for the 18.6 wt% $CaCO_3$ suspension.

Table 2. The values of ε_{ini}, p_{su} and p_{sb} at different $CaCO_3$ suspension concentrations

$CaCO_3$ conc. (wt%)	ε_{ini} (−)	p_{su} (Pa)	p_{sb} (Pa)
20.9	0.9146	1.32×10^{-2}	430.4
19.4	0.9211	3.25×10^{-3}	394.5
18.6	0.9245	1.53×10^{-3}	376.6
17.8	0.9278	6.93×10^{-4}	358.7
16.2	0.9345	1.24×10^{-4}	322.8
14.6	0.9414	1.78×10^{-5}	286.9
12.9	0.9483	1.95×10^{-6}	269.0
9.4	0.9625	6.92×10^{-9}	179.3
5.8	0.9772	1.16×10^{-12}	107.6

been calculated with only one theory.

3. Determination of the Value of p_{su} and p_{sb}

In the application of our hindered sedimentation theory, the solid compressive pressure of the solid blanket, p_{su}, and that of the bottom, p_{sb}, must be known.

To obtain the value of p_{su}, the initial porosity at the concentration, ε_{ini}, must be calculated. The ε_{ini} is calculated from the initial concentration of the suspension. When ε_{ini} is introduced into the constitutive equation, i.e., Eq. (1), the p_{su} is obtained.

p_{sb} is the solid compressive pressure of particle on the bottom, which is the gravitational force of the total particles minus the buoyancy force of the particles per total bottom area.

The initial porosity, ε_{ini}, the solid compressive pressure at the solid blanket, p_{su}, and the bottom solid compressive pressure, p_{sb}, are presented in Table 2.

The standard concentration of 18.6 wt% was marked with a partial gray background. The p_{su} calculated from initial suspension concentration, ε_{ini}, was assumed to be preserved during the entire sedimentation procedure.

At the moment sedimentation begins, all the particles in the suspension are subjected to p_{su}, even those on the bottom. However, the p_{sb} begins to increase thereafter. When the p_{sb} arrives at the total solid weight in the liquid per cell surface area, the driving force diminishes and the hindered sedimentation is complete. This means that the numerator in Eq. (4) is invalid, as is that of the sedimentation velocity.

The values of p_{su} and p_{sb} were observed to increase with increasing calcium carbonate suspension concentration. The value of p_{su} at the thinner concentration of 5.8 wt% was 1.16×10^{-12} Pa, which was small enough to be neglected. Therefore, the value of p_{su} can be neglected for thin suspensions. In the concentrated suspensions, 20.9 wt%, the calculation of the sedimentation procedure without p_{su} would not be accurate.

Herein, the whole procedure of hindered sedimentation was calculated with the p_{su} and p_{sb} values presented in Table 2.

4. Calculation of Hindered Sedimentation with Varying the Concentration of Suspension

Fig. 5 represents the sedimentation curves for various concentrations of calcium-carbonate suspension. The coefficients for the sedimentation theory are those values given in Tables 1 and 2.

In Fig. 5, the x-axis is the value of the sedimentation time (t) divided by the initial height (H_o), and the y-axis is the sedimentation

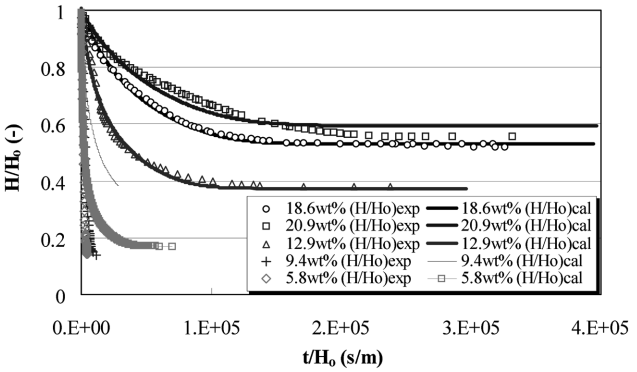

Fig. 5. Experimental and theoretical results of hindered sedimentation (5.8 to 20.9 wt% $CaCO_3$ suspensions).

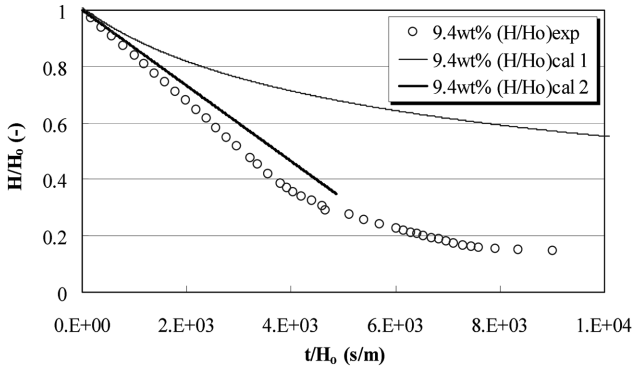

Fig. 6. Sedimentation for the 9.4 wt% $CaCO_3$ suspension.

height divided by the initial height (H_o). The white small points represents the experimental results of the 18.6 wt% calcium carbonate suspension. On the whole, the experimental and theoretical results coincided. Unlike the other theories, the entire hindered sedimentation procedure, from beginning to the end, can be calculated with our theory alone.

From these results, it is possible to confirm our hypotheses on hindered sedimentation, as below:

First, the force is transmitted by the contact of particles during hindered sedimentation.

Second, hindered sedimentation can be defined as the procedure where the solid compressive pressure at the bottom, p_{sb}, changes from a very small p_{su} to that of the total solid weight in the liquid per sedimentation area. Third, the whole sedimentation procedure can be calculated by using Darcy's equation, with variation of the average specific resistance based on the change of p_{sb}.

The concordance of the experimental and theoretical sedimentation results for the 20.9 wt% suspension was poor. During the first half, the height of the solid blanket was a little higher than that calculated theoretically. In our opinion, the frictional force between the particles and cell wall caused by the thick concentration retarded the sedimentation velocity. This phenomenon is the so-called "bridging effect," which is not contained within our theory.

The sedimentation curve for 12.9 wt%, as shown in Fig. 5, indicates good coincidence between the experimental and theoretical results.

However, the experimental results for the lower concentrations in the same figure, i.e., 9.4 and 5.8 wt%, are very different from the theoretical calculations (The solid blanket was not formed for suspensions below 5.8 wt%).

Although the 9.4 wt% concentration is not that different from 12.9 wt%, a huge discrepancy exists between the experimental and theoretical results. Our conclusion is that fundamentally, the sedimentation of 9.4 and 12.9 wt% suspensions do not have the same mechanism.

The basic notion used in this study was that the force is transmitted by the contact of particles during hindered sedimentation. As shown in Eq. (2), the total weight of particles in the liquid does act as the driving force for sedimentation. The weight is partially supported by the particles below, and this supporting force increases as hindered sedimentation proceeds. The decrease in this driving force results in a slowing of the sedimentation velocity.

Table 3. The values of and with changes in the $CaCO_3$ concentration

$CaCO_3$ conc. (wt%)	v_o (m/s)	α_{av} (m/kg)
20.9	9.47×10^{-6}	6.32×10^{8}
18.6	1.47×10^{-5}	4.07×10^{8}
12.9	2.05×10^{-5}	2.92×10^{8}
9.4	1.63×10^{-4}	3.67×10^{7}
5.8	2.73×10^{-4}	2.19×10^{7}

When the concentration of particles is too small for contact to occur, the transmission of force between the particles will disappear. In other words, the supporting force in the numerator of Eq. (2) and the p_{sb} in Eq. (4) will become negligible. As a consequence, the sedimentation velocity becomes very fast, as expected, Eqs. (2) and (4). The calculation for the 9.4 wt% suspension using this concept is shown in Fig. 6 as "calculation 2," which is indicated by the thick line. The thin line represents the calculated result based on the transmitting forces. These two lines are very different.

The thick line does not coincide perfectly with experimental results, which was thought to be as a result of the difference in the particle size distribution.

Table 3, shows the sedimentation velocity and average specific resistance for various sedimentation concentrations.

The sedimentation velocity increases as the concentration of suspensions becomes thinner. The sedimentation velocity of the 18.6 wt% suspension was 1.47×10^{-5} m/s, and that of 12.9 wt% was 2.05×10^{-5} m/s; thus a 1.4 times increase in the sedimentation velocity. The sedimentation velocities of the 9.4 and 5.8 wt% suspension, for which our theory does not apply, were 1.63×10^{-4} and 2.73×10^{-4} m/s, respectively, which are 11 and 18.6 times faster, respectively, than that of the 18.6 wt% suspension. This is where the greatest difference exists; the average specific resistances were also very different for 9.4 and 5.8 wt% suspension, for which our theory does not apply.

The difference between the experimental and theoretically calculated results for suspensions with very low concentrations could possibly be proof of the appropriateness of our theory. Tiller et al. [2000] proposed the 'critical volumetric solid concentration,' and insisted that the (effective) solid compressive pressure was zero for sedimentation heights greater than the critical volumetric solid con-

centration. From their experiments, the critical volumetric solid concentration of a kaolin suspension was determined to be 0.07, corresponding to 16.2 wt%. The lower limit of our theory for calcium carbonate suspensions was between 12.9 and 9.4 wt%, indicating similar conceptual and experimental results.

From the experimental and theoretically calculated results, hindered sedimentation can be divided into two mechanisms.

First, hindered sedimentation of high concentrations, during which contact between particles and the transmission of solid compressive pressure exist, where a definite solid blanket appears and the whole sedimentation procedure can be explained and calculated.

Second, hindered sedimentation without transmission of solid compressive pressure at relatively low concentrations. The sedimentation velocity is very fast compared to the first case. When the only purpose is that of fast sedimentation, the operation at this concentration is recommended.

5. Distribution of Porosity During Hindered Sedimentation

The local porosities are calculated to find the variation in the sedimentation bed during the operation. Using the concept of Tiller and Cooper [1962], the relation between position x and the solid compressive pressure can be expressed as:

$$\frac{x}{L} = \left(\frac{p_s}{p}\right)^{1-n-\beta} \tag{10}$$

where, x/L is the ratio of the sedimentation height, with 0 referring to the bottom of sedimentation cell, and 1 to the solid blanket. Substituting our boundary conditions of hindered sedimentation into Eq. (10), Eq. (11) is obtained:

$$\frac{x}{L} = \frac{p_s^{1-n-\beta} - p_{sb}^{1-n-\beta}}{p_{su}^{1-n-\beta} - p_{sb}^{1-n-\beta}} \tag{11}$$

Rearranging Eq. (11) with respect to p_s, gives,

$$p_s = \left[\frac{x}{L} \times (p_{su}^{1-n-\beta} - p_{sb}^{1-n-\beta}) + p_{sb}^{1-n-\beta}\right]^{1/1-n-\beta} \tag{12}$$

The values for n and β obtained by the sedimentation results, as shown in Table 1, were used. The p_{su} and p_{sb} at the start and end of sedimentation were applied to Eq. (12) for individual sedimentation concentrations. Thus, the calculated p_s was introduced into Eq. (1) in this study to obtain the porosity at position, x/L.

The concentrations of 18.6, 20.9 and 12.9 wt%, which were chosen as the standard, and the higher and lower concentrations, respectively, were chosen for calculating the porosity distribution, and are shown in Figs. 7, 8 and 9.

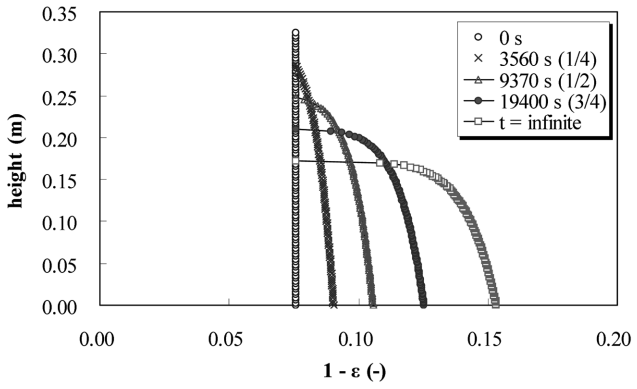

Fig. 7. The porosity and sedimentation height during sedimentation of the 18.6 wt% $CaCO_3$ suspension.

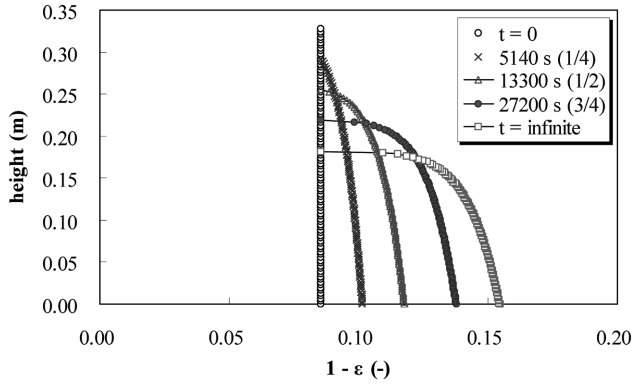

Fig. 8. The porosity and sedimentation height during sedimentation of the 20.9 wt% $CaCO_3$ suspension.

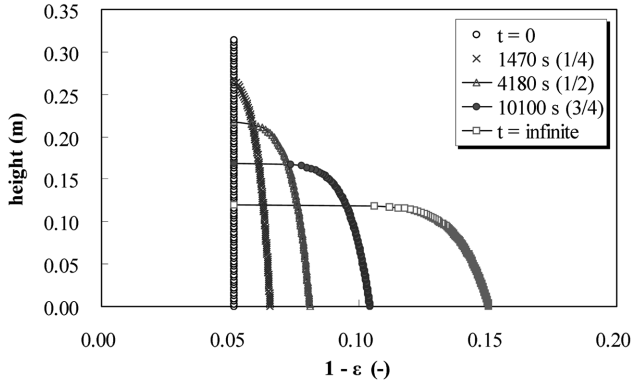

Fig. 9. The porosity and sedimentation height during sedimentation of the 12.9 wt% $CaCO_3$ suspension.

Figs. 7, 8 and 9 show the porosity distributions with on going sedimentation for 18.6, 20.9 and 12.9 wt% calcium carbonate suspensions, respectively. The x and y axes indicate $(1-\varepsilon)$ and the height of sedimentation, respectively.

In Fig. 7, the vertical white points at the left end indicate the porosity distribution at the start of sedimentation. The porosities were 0.924 for all sedimentation heights.

The second line composed of the x is the porosity distribution when the sedimentation is 3/4 of the original height, 3,560 seconds, having past.

The porosity distribution when the solid blanket was 1/2 the original height is shown by the third line constructed by the triangles. The time passed to achieve this height was 9370 seconds.

The fourth line of black points represents the porosity distribution at 1/4 of the original height, and final line of white squares is the porosity distribution at the end of sedimentation. The value of $(1-\varepsilon)$ at the bottom, i.e. x/L is zero, increases as sedimentation progresses, which is caused by the decrease in porosity due to piling of solid particles on the bottom. As a result, the value of $(1-\varepsilon)$ for x/L=0 and at infinite sedimentation time was calculated as 0.153, that is, a porosity of 0.837.

The explanation for hindered sedimentation from Fig. 7 is as fol-

Table 4. The values for the sedimentation height, sedimentation time and with changes in the $CaCO_3$ concentration

$CaCO_3$ suspension (wt%)	Sedimentation progress	Sedimentation height (m)	Sedimentation time (sec)	p_{sb} (Pa)
18.6	0	0.325	0	1.53×10^{-3}
	1/4	0.287	3,560	3.51×10^{-2}
	1/2	0.248	9,370	5.48×10^{-1}
	3/4	0.210	19,400	1.10×10^{1}
20.9	0	0.328	0	1.32×10^{-2}
	1/4	0.292	5,140	2.67×10^{-1}
	1/2	0.255	13,300	3.58×10^{0}
	3/4	0.219	27,200	5.69×10^{1}
12.9	0	0.314	0	1.95×10^{-6}
	1/4	0.266	1,470	1.26×10^{-4}
	1/2	0.217	4,180	0.50×10^{-2}
	3/4	0.169	10,100	4.33×10^{-1}

lows. At the initiation of hindered sedimentation, all particles composing the suspension receive the same value of p_{su}. Therefore, the particles on the bottom also receive the same values of p_{su} which is the smallest solid compressive pressure in the course of the procedure.

As the porosity for a given moment was calculated by the smallest p_{su} using constitutive Eq. (1), the porosity at that moment has the largest value, and will be constant throughout the entire cell.

Calculations of a same manner were performed for two different concentrations, and the results are shown in Figs. 8 and 9. These figures have almost the same trend, differing only in that the higher concentration gave a higher initial $(1-\varepsilon)$ values. It is interesting that the higher concentration did not give a much higher $(1-\varepsilon)$ value at the bottom after complete sedimentation.

Figs. 7 to 9, can be used to easily verify the variations in the porosity during the progression of hindered sedimentation.

To more clearly explain Figs. 7 to 9, the sedimentation height and time, and the solid compressive pressure at the bottom p_{sb} for a certain degree of sedimentation for various concentrations are shown in Table 4.

The initial height of the solid blanket at the start of sedimentation with the 18.6 wt% suspension was 0.325 m, with the of 1.53×10^{-3} Pa being the same as that of p_{su}. At the little higher concentration of 20.9 wt%, the initial height was 0.328 m, with a value of p_{sb} of 1.32×10^{-2} Pa, which was slightly higher than that for 18.6 wt% suspension. At a lower concentration of 12.9 wt%, the initial height was 0.314 m, with a p_{sb} of 1.95×10^{-6} Pa, the lowest pressure obtained. As the sedimentation progressed, the solid compressive force on the bottom p_{sb} increased. The value of p_{sb} increased faster with higher suspension concentrations. The time needed for to obtain a height of x/L=3/4 was 27,200 seconds (about 7 and half hour) for the 20.9 wt% calcium carbonate suspension.

CONCLUSION

Herein, a new hindered sedimentation theory which can calculate the whole hindered sedimentation procedure, based on the "unified theory of solid-liquid separation" has been proposed. The coefficients a, n, B and β, used in the calculations were decided upon by experiments using the CPC (compression-permeability cell) and sedimentation. The solid compressive pressure at the solid blanket, p_{su}, and that at the bottom, p_{sb}, were calculated, and utilized as the boundary conditions. The experiments and calculations for calcium carbonate suspensions were performed at concentrations between 5.8 to 20.9 wt%. A comparison of the experimental and calculated results, gave a lower limit of our hindered sedimentation theory for a calcium carbonate suspension between 12.9 and 9.4 wt%. The porosity distribution during hindered sedimentation was calculated, and the porosity variation theoretically analyzed from the results.

ACKNOWLEDGMENT

This work was supported by INHA UNIVERSITY Research Grant.

REFERENCES

Alan, S. M. and Justin, C. B., "Settling Rates and Sedimentation Volumes of Flocculated Kaolin Suspensions," *I. & E.C. Fundamentals*, **1**, 25 (1962).

Burger, R., Concha, F. and Tiller, F. M., "Applications of the Phenomenological Theory to Several Published Experimental Cases of Sedimentation Processes," *Chemical Engineering Journal*, **80**, 105 (2000).

Grace, H. P., "Resistance and Compressibility of Filter Cakes. Part I," *Chemical Engineering Progress*, **49**, 303 (1953).

Kynch, G. J., "A Theory of Sedimentation," *Trans. Faraday Assoc.*, **48**, 166 (1952).

Maude, A. D. and Whitmore, R. L., "A Generalized Theory of Sedimentation," *J. Appl. Phs. (Br.)*, **9**, 477 (1958).

McCabe, W. L., Smith, J. C. and Harriott, P., *Unit Operations of Chemical Engineering*, 5th ed., McGraw-Hill Book Co., New York, NY (1995).

Richardson, J. F. and Zaki, W. N., "Sedimentation and Fluidization : Part I," *Trans. Inst. Chem. Engrs.*, **32**, 32 (1954).

Ruth, B. F., "Correlating Filtration Theory with Industrial Practice," *Industrial and Engineering Chemistry*, **38**, 564 (1946).

Tiller, F. M. and Cooper, H., "The Role of Porosity in Filtration: Part V. Porosity Variation in Filter Cakes," *AIChE J.*, **8**, 445 (1962).

Tiller, F. M. and Crump, J. R., "Solid-Liquid Separation : An Overview," *CEP*, 65 (1977).

Tiller, F. M. and Horng, L. L., "Hydraulic Deliquoring of Compressible Filter Cakes," *AIChE J.*, **29**, 297 (1983).

Tiller, F. M. and Khatib, Z., "The Theory of Sediment Volumes of Compressible, Particulate Structures," *Journal of Colloid and Interface Science*, **100**, 55 (1984).

Yim, S. S. and Kwon, Y. D., "A Unified Theory on Solid-Liquid Separation: Filtration, Expression, Sedimentation, Filtration by Centrifugal Force, and Cross Flow Filtration," *Korean J. Chem. Eng.*, **14**, 354 (1997).

Yim, S. S., Song, Y. M. and Kwon, Y. D., "The Role of P_i, P_a, and P_f in Constitutive Equation, and Boundary Condition in Cake Filtration," *Korean J. Chem. Eng.*, **20**, 334 (2003).

Yim, S. S., Song, Y. M. and Lee, J. Y., "New Expression Theory Based on Darcy's Equation: Unified Theory on Solid-Liquid Separation," *Korean Chem. Eng. Res.*, **41**, 471 (2003).